Temperature-dependent Urbach tail measurements of CaF_2 single crystals

M. Letz,[1] A. Gottwald,[2] M. Richter,[2] and L. Parthier[3]
[1]*Schott AG, Research and Development, D-55014 Mainz, Germany*
[2]*Physikalisch-Technische Bundesanstalt, D-10587 Berlin, Germany*
[3]*Schott Lithotec AG, Otto-Schott Strasse 13, D-07745 Jena, Germany*
(Received 12 February 2009; published 14 May 2009)

In the deep ultraviolet spectral range the transmission of high-purity CaF_2 was measured using synchrotron radiation. In the vicinity of the band gap below 11.2 eV or for wavelength longer than 90 nm, a scaling behavior of the absorption as a function of photon energy was observed. Temperature-dependent measurements allow one to distinguish two different absorption mechanisms which differ by their ability to couple to phonon excitations. These two types of Urbach tails were analyzed. The origin of the temperature-independent tail is due to defects in the lattice, whereas the temperature-dependent part originates from short-time localization of exciton mode coupling to lattice distortion.

DOI: 10.1103/PhysRevB.79.195112 PACS number(s): 78.40.−q, 71.35.−y, 78.70.−g, 81.16.Nd

I. INTRODUCTION

Single crystals of calcium fluoride (CaF_2) are widely used for their superior optical properties. In the infrared spectral region, the material is transparent and very stable under intense laser radiation up to a wavelength of 10 μm (or 0.1 eV of photon energy). In the ultraviolet (UV) spectral range it is transparent down to 125 nm. Therefore, CaF_2 is a highly important material for optical components in lithographic processes, e.g., used for industrial semiconductor manufacturing. The smallest possible structure size which can be obtained by the microlithographic process is proportional to the wavelength of the radiation used for structuring. During the last years, immense effort has been made in order to provide large single crystals of CaF_2 with high optical quality. The microlithographic processes are performed at wavelengths of excimer laser radiation sources in the deep ultraviolet (DUV) spectral range, mainly at 193 nm by ArF excimer lasers. CaF_2 is chosen as an optical material due to its cubic crystal structure with nearly[1,2] perfect optical isotropy, due to its chemical durability, and due to its mechanical properties which makes it applicable for lens fabrication.

Recently, the 193 nm (or 6.43 eV) lithography got extended into industrial mass applications to address the 45 nm node for semiconductor structuring using water as an immersion fluid. Further increase in resolution is planned by applying fluids with higher refractive indices. A "node" is half the minimum distance between the centers of the two parallel adjacent wires structured on a silicon chip using the microlithographic technique. The driving force of the semiconductor industry led to the development of high-quality extremely pure crystals of CaF_2.

In the present paper we focus on the transparency of the material in the DUV part of the spectral range, where particular absorption mechanisms can be observed. Especially, close to the band gap (for photon energies smaller than 11.2 eV or wavelengths longer than 90 nm), scaling laws can be observed. We investigated these so-called Urbach tails and distinguished between different absorption mechanisms by measuring the temperature dependence of the absorptions. Also these mechanisms are already known for a long time; these investigations are experimentally more detailed and only possibly due to the recent availability of highly pure CaF_2 crystals in the context of material development for microlithography.

II. EXPERIMENT

The measurements were performed at the UV and VUV beamlines for detector calibration and reflectometry in the laboratory of the Physikalisch-Technische Bundesanstalt at the electron storage ring BESSY II.[3] The beamline supplied radiation with high spectral purity achieved by optimized coatings and grating constants for different spectral subranges and use of various bulk filters for higher-order suppression. The spot size in focus amounted to 1 mm vertical by 3 mm horizontal at a spectral resolution of 1.7 nm. Within the bandwidth, the typical radiant power amounted from some hundred nanowatts for stored ring currents of 100 mA. The wavelength scale at the beamline was determined using a spectral lamp, and in addition, rare-gas absorption resonances. The overall wavelength uncertainty was 0.1 nm, while the reproducibility of the wavelength was better than 0.05 nm.

An ultra-high-purity CaF_2 sample was supplied from Schott Lithotec. In a reflectometer, the transmittance of the samples was measured in a near-normal-incidence geometry for different sample temperatures ranging between −50 °C (223 K) and 80 °C (353 K). The incoming beam of synchrotron radiation, spectrally dispersed by a normal-incidence monochromator, as well as the reflected beam was measured by the same semiconductor photodiode. The monochromator allowed continuous tuning of the wavelength from 40 to 400 nm. In order to enhance the spectral purity of the beam, an argon gas cell was used to suppress higher diffraction orders from the monochromator grating. The measurements were performed by embedding the reflection measurements of the samples into two reference measurements of the incoming beam intensity. Online monitoring allowed normalization to variations in the beam intensities. For temperature selection and control, a specific sample holder was used, which al

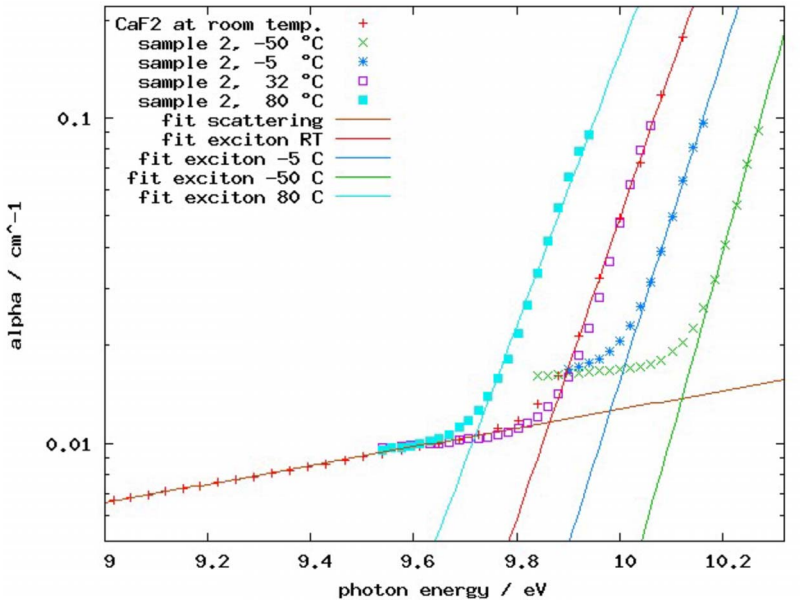

FIG. 1. (Color online) The extinction coefficient restricted to the small region of the present measured data of CaF_2 is plotted on a logarithmic scale as a function of photon energy.

lowed one to change the sample temperature between 223 and 355 K.[4] The sample holder was cooled by liquid nitrogen and heated by Peltier elements. It was thermally connected to a cryostat (as heat sink) by a copper cord. Two Peltier elements were mounted between the copper cord from the heat sink and the sample holder. The temperature was stabilized by an electronic feedback control unit. The stabilization typically took about 10 min before thermal equilibrium on the sample holder was achieved, monitored by PT100 thermometers on the sample.

The sample we used was a high-purity, tempered, and cleaved CaF_2 crystal with surface normals pointing in the [111] directions. The sample thickness was 9.5 mm. We measured the dependence of the absorption of the sample as a function of photon energy and temperature. The result is shown in Fig. 1. One can clearly see the different parts of the Urbach tail. On a logarithmic scale the extinction coefficient α is plotted as a function of photon energy. When measuring at different temperatures, two regimes can clearly be distinguished. In the first regime, ln α increases linearly with increasing photon energy but is not temperature dependent. This regime dominates in the CaF_2 samples under investigation for photon energies up to around 9.5 eV. However, for photon energies above 9.5 eV, a strongly temperature-dependent contribution to the Urbach tail dominates. This is shown in Fig. 1 for five different sample temperatures. Heating of the material decreases the band gap, which is seen for the data obtained at 80 °C, whereas cooling increases the band gap, which is seen for the results obtained for −5 °C and −50 °C. The temperature-independent offset of the −5 °C and the −50 °C results is due to absorptions of condensates on the sample surfaces. In Fig. 2 we plot the whole energy range to the band gap which is known from reflection measurements and show the expected scaling. We know from reflection measurements on oriented surfaces[2] that the true band gap is dominated by the exciton at 11.2 eV.

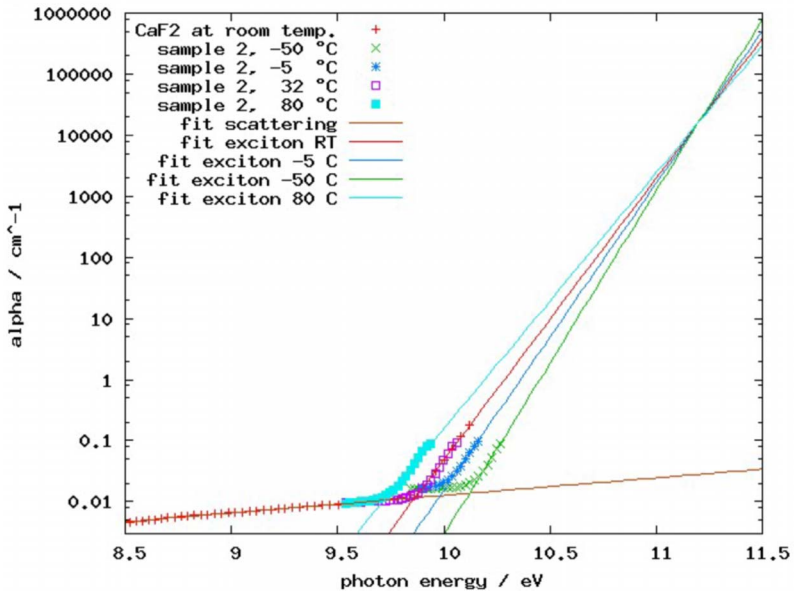

FIG. 2. (Color online) The scaling of the data to the intrinsic band gap of CaF_2; the Γ exciton at 11.2 eV is shown.

III. LOSS MECHANISMS AND URBACH TAIL

In an ideal perfectly insulating single crystal, completely free of defects and at zero temperature, the first optical excitation is expected to occur at the photon energy where the radiation creates electron-hole pairs. Such electron-hole pairs can, on one hand, exist as free unbound single electrons and holes by excitation into the one-particle continuum above the band gap. On the other hand, in a strongly ionic system such as a halogenide crystal, there is the possibility to excite into a two-particle bound state of the electron and the hole: the exciton. In CaF_2, the Γ exciton is known to be at a photon energy of 11.2 eV (Refs. 5 and 6) and the single-particle (unbound) continuum starts around 11.8 eV. We believe that the relevant first absorption belongs to the Γ exciton since we do not observe a temperature-dependent decrease in the exciton resonance in the reflection spectrum which would indicate an indirect transfer with a finite momentum. Our interpretation differs from the one in Ref. 6 which interpreted it as an $X_5' \rightarrow X_3$ exciton. Such an indirect transfer is in principle possible in CaF_2 since the minimum of the band gap is indirect, having a minimum by exciting a pair of a Γ hole and an X electron. A calculation of the relevant absorptions can be found in Ref. 7. Real systems, however, are neither free of defects nor used at zero absolute temperature. Therefore, we have to discuss further absorption mechanisms.

First of all, there is an extrinsic loss mechanism due to disorder in the lattice. The most common type of defects in real crystals is ion impurities, which are point defects leading to localized electronic impurity states close to the band gap. In CaF_2 with a lattice constant of 0.43 nm, 1 ppb of impurities means already that the average distance between neighboring impurities is $\sqrt[3]{10^6(0.43\ \text{nm})^3}=43$ nm which is already much smaller than the wavelength used in DUV lithography. Another mechanism leads to defects even if one would have an ideal material, free of impurities, which has never come in contact with any crucible of a different material. This mechanism is based on the fact that crystal growth does not take place at zero absolute temperature but around the melting point of the crystal which is about 1500 K for CaF_2. Therefore entropy will already introduce a number of intrinsic defects such as F^- vacancies, F interstitials, and grain boundaries. Also these defects will lead to localized electronic states close to the band gap. A third mechanism is related to temporarily trapping of excitons in lattice distortions. Theoretical explanations, e.g., by Ihm and Phillips,[8] John *et al.*,[9] and Schmitt-Rink *et al.*,[10] mostly refer to the work of Toyozawa,[11,12] who described a temporarily trapping of excitons, and later to Dow and Redfield in a series of papers,[13–15] who described a model of field ionized excitons. Both models point out that understanding the interaction between the exciton and other elementary excitations is the crucial point to explain the shape and temperature dependence of the Urbach tails. As already mentioned, radiation interacts in a solid by creating electron-hole pairs. In strongly ionic solids such as CaF_2, screening of the Coulomb interaction between electron and hole by mobile charge carriers is not too strong. In this case the effective interaction is strong enough for an electron-hole pair to form a two-particle bound state with a somewhat lower energy, which then is the exciton. Following the ideas of Toyozawa,[11] such electron-hole pairs can further lower the electronic energy, which is needed to excite them by interacting with a lattice distortion. The larger the temperature is, the more lattice distortions in form of phonon modes are available. We can understand this phenomenon as electron-hole pairs, which virtually and temporarily jump into a lattice distortion and back. During the time when the electron-hole is in the lattice distortion, the photon energy needed for an excitation can be reduced, which leads to absorptions below the threshold of the bare exciton, i.e., below 11.2 eV for CaF_2.

For insulators, there exist a very universal scaling of the extinction coefficient around the band gap called the Urbach (or Urbach-Martiensen) tail.[16,17] It has the general form

$$\alpha_1(\omega) = \alpha_0 e^{A(\hbar\omega - E_0)}, \tag{1}$$

where E_0 is the energy of the band gap at zero temperature, $\omega=2\pi\nu=2\pi c/\lambda$ is the angular frequency, $\hbar$ the Planck constant, and α_0 and A are the fit parameters. Despite numerous efforts in theoretical understanding no consistent quantitative microscopic model exists, which gives a clear physical interpretation of the fit parameters. We might understand a_0 as the average absorption cross section of a local defect multiplied with the overall effective defect concentration. The exponential function is then the probability to find a defect level an energy $\Delta E=E_0-\hbar\omega$ below the band gap. For a strongly ionic system with a close to perfect periodicity such as high-quality single crystals of large band-gap insulators, the dominant mechanism for the states just below the band gap is the exciton localization due to exciton-phonon interaction. This means that the exciton, which is usually delocalized and shows a particular dispersion, can be temporarily localized due to the interaction with (optical) phonon modes. Since the number of available phonons is a function of temperature, parameter A shows for ionic insulators at sufficiently large temperatures a well-defined temperature dependence,

$$\alpha_2(\omega) = \beta_0 e^{\sigma e(\hbar\omega - E_0)/k_B T}, \tag{2}$$

where k_B is the Boltzmann constant, σ is a new fit parameter, and e is the electron charge. For common insulators[18] such as CuCl or TlCl the parameter α_0 is of the order of 3×10^4 cm^{-1} and σ is of the order of unity. The total absorbance α, then, is given as the sum $\alpha_1+\alpha_2$. Also for the temperature-dependent fit function no satisfying quantitative microscopic theory exists. We can understand β_0 as the absorption of the exciton and the exponential function as the probability to localize an exciton in a lattice distortion $\Delta E=E_0-\hbar\omega$ below the band gap. The factor σ should be of order unity. The probability to find such a lattice distortion strongly increases with temperature due to more phonon modes in the phonon density of states which become occupied with increasing temperature. The model of Dow and Redfield[13–15] relate the probability to the optical phonon frequency Ω_0 by introducing an effective temperature,

$$T \to T^* = \frac{\hbar\Omega_0}{2k_B}\coth\frac{\hbar\Omega_0}{2k_BT}. \quad (3)$$

In this way they are able to describe the different scaling laws which are found in ionic and covalent insulator materials. In our case of CaF_2 we have a strongly ionic insulator which should show just the exponential temperature dependence.

IV. FIT TO EXPERIMENTAL DATA

With regard to the formalism discussed above, we can now fit the temperature-independent as well as the temperature-dependent part of the Urbach tail. For the temperature-independent part we obtain for the parameters of Eq. (1) using $E_0 = 11.2$ eV,

$$\alpha_1(\omega) = \alpha_0 e^{A(\hbar\omega - E_0)},$$

$$\alpha_0 = 0.28 \ \text{cm}^{-1},$$

$$A = 0.66 \ \text{eV}^{-1}, \quad (4)$$

where the photon energy is measured in units of eV. The temperature-dependent part of the Urbach tail is fitted using Eq. (2) with

$$\alpha_2(\omega) = \beta_0 e^{\sigma e(\hbar\omega - E_0)/k_BT},$$

$$\beta_0 = 0.097 \ \text{cm}^{-1},$$

$$\sigma = 0.29 \pm 0.05, \quad (5)$$

where $\frac{k_BT}{e}$ is the temperature measured in units of eV and e is the electron charge. In the inset of Fig. 1 we have plotted the whole fit up to the crossing point at 11.2 eV. In the main plot of Fig. 1 only the area where measured data exist is shown in detail.

We interpret our results as follows. In the temperature-independent part of the Urbach tail, the absorption is dominated by extrinsic defects such as impurity ions or imperfections in the crystal structure such as grain boundaries. All these crystal imperfections lead to electronic (localized) states within the band gap and give rise to the temperature-independent contribution. We interpret the temperature-dependent part as the temporary trapping of excitons in lattice distortions. While the trapping of an exciton in a lattice distortion costs energy the electronic energy to excite an electron-hole pair is lowered, leading to a number of states below the band gap, which can be excited with electromagnetic radiation. The larger the temperature is, the more lattice distortions are present. Therefore, with increasing temperature the absorption around the band gap increases. This is clearly observed in our temperature-dependent measurements.

V. CONCLUSION

On one hand we have the development of ultrapure material for the need of the semiconductor industry. On the other hand the radiation source of the Physikalisch-Technische Bundesanstalt in Berlin with its excellent beam quality allows highly accurate measurements. The combination of these two gives deep insight into the scaling laws in the vicinity of the band gap. CaF_2 as a strongly ionic insulator with deep exciton bound states and a wide band gap is an extreme case to test theories for scaling laws below the band gap. It represents a material where clearly exciton effects dominate. The excitation of unbound electrons-hole pairs plays a minor role here. Overall we have shown that it is possible to separate the Urbach tail in a temperature-dependent and a temperature-independent one. We associate the latter with extrinsic impurities in the crystal. We interpret the temperature-dependent part via an interaction between optical phonon modes and excitons.

[1] J. H. Burnett, Z. H. Levine, and E. L. Shirley, Phys. Rev. B **64**, 241102(R) (2001).
[2] M. Letz, L. Parthier, A. Gottwald, and M. Richter, Phys. Rev. B **67**, 233101 (2003).
[3] M. Richter, J. Hollandt, U. Kroth, W. Paustian, H. Rabus, R. Thornagel, and G. Ulm, Metrologia **40**, S107 (2003).
[4] A. Gottwald, U. Kroth, M. Letz, H. Schöppe, and M. Richter, Proc. SPIE **5538**, 157 (2004).
[5] T. Tomiki and T. Miyata, J. Phys. Soc. Jpn. **27**, 658 (1969).
[6] J. Frandon, B. Lahaye, and F. Pradal, Phys. Status Solidi B **53**, 565 (1972).
[7] L. X. Benedict and E. L. Shirley, Phys. Rev. B **59**, 5441 (1999).
[8] J. Ihm and J. C. Phillips, Phys. Rev. B **27**, 7803 (1983).
[9] S. John, C. Soukoulis, M. H. Cohen, and E. N. Economou, Phys. Rev. Lett. **57**, 1777 (1986).
[10] S. Schmitt-Rink, H. Haug, and E. Mohler, Phys. Rev. B **24**, 6043 (1981).
[11] Y. Toyozawa, Prog. Theor. Phys. **20**, 53 (1958).
[12] Y. Toyozawa, Prog. Theor. Phys. **22**, 455 (1959).
[13] J. D. Dow and D. Redfield, Phys. Rev. B **1**, 3358 (1970).
[14] J. D. Dow and D. Redfield, Phys. Rev. Lett. **26**, 762 (1971).
[15] J. D. Dow and D. Redfield, Phys. Rev. B **5**, 594 (1972).
[16] F. Urbach, Phys. Rev. **92**, 1324 (1953).
[17] W. Martienssen, J. Phys. Chem. Solids **2**, 257 (1957).
[18] E. Mohler and B. Thomas, Phys. Rev. Lett. **44**, 543 (1980).